IEEE Photonics Journal
An IEEE Photonics Society Publication

Open Access

Long-Period Fiber Grating Within D-Shaped Fiber Using Magnetic Fluid for Magnetic-Field Detection

Volume 4, Number 6, December 2012

Lei Gao
Tao Zhu, Member, IEEE
Ming Deng
Kin Seng Chiang
Xiaokang Sun
Xiaopeng Dong
Yusong Hou

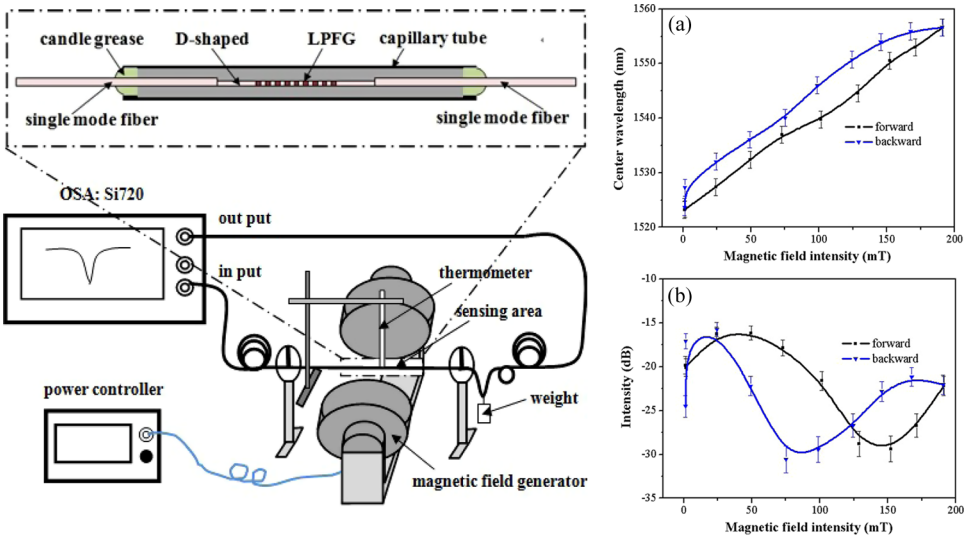

DOI: 10.1109/JPHOT.2012.2226439
1943-0655/$31.00 ©2012 IEEE

Long-Period Fiber Grating Within D-Shaped Fiber Using Magnetic Fluid for Magnetic-Field Detection

Lei Gao,[1] Tao Zhu,[1] *Member, IEEE*, Ming Deng,[1] Kin Seng Chiang,[2] Xiaokang Sun,[1] Xiaopeng Dong,[3] and Yusong Hou[1]

[1]Key Laboratory of Optoelectronic Technology & Systems (Ministry of Education), Chongqing University, Chongqing 400044, China
[2]Department of Electronic Engineering, City University of Hong Kong, Kowloon, Hong Kong
[3]Department of Electronic Engineering, Xiamen University, Fujian 361000, China

DOI: 10.1109/JPHOT.2012.2226439

Manuscript received September 25, 2012; revised October 18, 2012; accepted October 19, 2012. Date of publication October 24, 2012; date of current version November 15, 2012. Corresponding author: T. Zhu (e-mail: zhutao@cqu.edu.cn).

Abstract: A magnetic sensor utilizing long-period fiber grating (LPFG) written by high frequency CO_2 laser pulses in a D-shaped fiber and the magneto-optical effect of magnetic fluid is proposed. Because of the high evanescent field of the grating structure in D-shaped fiber, by immersing the LPFG with a period of 685 μm into a water-based magnetic fluid within a capillary tube, the redshift as high as 33.5 nm of the resonant wavelength of the grating is observed when the external magnetic-field intensity is 189.7 mT, resulting in a sensitivity of 176.4 pm/mT. The hysteresis effect is observed and explained by the characters of magnetic fluid. Such kind of sensors would find potential applications in magnetic sensing fields.

Index Terms: Sensors, fiber gratings, light–material interactions.

1. Introduction

Magnetic-field sensing is very important to the industry of military, aviation, controlled nuclear fusion, and biomedical detection [1], [2]. Compared with the traditional magnetic sensors, which are in large size and influenced by electromagnetic interference easily [2], optic-based technology has outstanding merits in magnetic sensing, as it is insulated and light weighted as sensors or carriers [3], [4]. Optical fiber has various potential applications on monitoring magnetic field due to its simple structure, high temperature resistance, immunity of electromagnetic interference, corrosion resistance, and easy multiplexing abilities [5]. With the development of kinds of new materials, fiber-based technology brings more and more developing spaces for magnetic sensing [6].

The main factors of fiber-based magnetic sensors are determined by the magneto-optical effect of materials, such as magnetic fluid (MF) and magnetic-strict materials [7]. In addition, the output intensity of interferometer or resonant wavelength of grating will vary from different magnetic-field intensity caused by different sensing mechanism, such as Mach–Zehnde interferometer or grating [8], [9]. Okamura has designed a magnetic sensor based on Lorentzian force on one arm of Mach–Zehnder interferometer to obtain the optical phase sensitivities of 0.11 rad/(A/m) for dc magnetic field by using 100 mm of Al-coated sensor fiber [8]. A tunable optical filter based on fiber Bragg grating (FBG) and Faraday effect was proposed to be used as magnetic-field intensity sensor [10], which has the sensitivity of 6.7 $\times$ 10-4 pm/mT. Liu *et al.* proposed a magneto-optical tunable

filter based on long-period fiber grating (LPFG) coated with MF as the ambient media. As the refractive index (RI) of MF depends on the external magnetic-field intensity, then the resonant wavelength of LPFG shifts with variation of the external magnetic field. If the tuning of magnetic field is from 0 to 1661 Oe (0 $\sim$ 166.1 mT), the resonant wavelength of LPFG will shift to longer wavelength up to 7.4 nm [9]. Meanwhile, based on the magneto-optical property, Thakur *et al.* reported a magnetic-field sensor by injecting MF into the cladding holes of a polarization-maintaining photonic crystal fiber (PM-PCF), resulting in a sensitivity of 242 pm/mT [11]. However, it is hard to detect magnetic field in small area, for the length of the PM-PCF is 23.5 cm. Zu *et al.* proposed a loop consisting of a Sagnac interferometer, a MF film, and a section of polarization-maintaining fiber to produce a sinusoidal interference spectrum for magnetic-field measurement, resulting in a sensitivity of 167 pm/mT [12]. And the experimental results were presented by Konstantaki *et al.* on spectral tuning of LPFG utilizing water- and oil-based MF as the exterior cladding, and changes of 7.5 nm and 6.5 dB were monitored in the resonant wavelength and the attenuation band contrast for the water-based MF, respectively. By repeating the changes of the magnetic-field intensity, the hysteresis effect was clear to be observed. Then, the attenuation band contrast of the LPFG was modified by more than 10%, while there is no change for its resonant wavelength position [13].

Evanescent field is fascinating for its high energy conductivity, which could be used to enhance the sensing sensitivity. Striping the fiber cladding or drawing the fiber into micrometers [14], [15], even in nanometers in diameter, it is still available to enlarge the evanescent field [16]. Based on the tuning capabilities of the propagation characteristics of optical modes, different kinds of optofluidic tunable fibers were presented [17]. Pu *et al.* has reported that, when an MF modulator is used as the cladding of drawn fiber, the light intensity guiding in the fiber would alternate with the changes of magnetic-field intensity [15]. However, the microfibers is fragile due to the diameter of the uniform waist is only about 19.3 μm.

Removing part of the cladding with etching or polishing [18], it is easy to know that D-shaped fiber is more effective to enlarge evanescent field by a higher fraction of the guiding mode interacting directly with the surroundings; meanwhile, the mechanical strength of fiber remains well [19]. Kim *et al.* fabricated LPFG on a D-shaped PCF formed by side polishing through the spin-coating and standard contact lithography, then wavelength shifted 122 nm when RI unit (RIU) of the RI changed from 1 to 1.45 [20]. Chen *et al.* proposed an optical sensor based on LPFG ultraviolet inscribed in D-shaped fiber [19], with sensitivity enhancement by cladding etching and the surroundings RI ranging from 1.33 to 1.40 leading to the shifts of 31.7 nm and 13.8 nm for the etched and nonetched cases, respectively. Tien *et al.* coated the polished surface of the LPFG with iron thin film to function as a sensing head [21], and an nonlinear relation between the wavelength shift and magnetic field was obtained, leading to the maximum wavelength shift of 36 nm in the case of a magnetic field of 153 KA/m (191.25 mT). However, the nonlinear responsibility and more measurement range of magnetic should be improved.

In this paper, we have investigated the LPFG in a D-shaped fiber written by high-frequency CO_2 laser pulses [22]–[24]. By immersing the LPFG in water-based MF within a capillary tube, the transmission spectra are measured while the applied magnetic-field intensity changed. We have demonstrated that the magnetic-field sensitivity of the device is very high and clarified why it has high sensitivity in detail; meanwhile, we have investigated the attenuation band contrast of the grating immersed in MF. Finally, the hysteresis effect are observed and explained with the characters of the MF.

2. Sensing Principle

LPFG is a transmission grating, in which the coupling is between modes traveling in the same direction, which is couples light from the core mode into the cladding modes at specific wavelengths, yielding corresponding attenuation bands for transmission spectrum [25]. The resonant wavelength λ_i of the *i*th attenuation band is given by the phase matching condition

$$\lambda_i = \left[n_{co}^{eff}(\lambda_i) - n_{cl}^{eff}(\lambda_i)\right]\Lambda \tag{1}$$

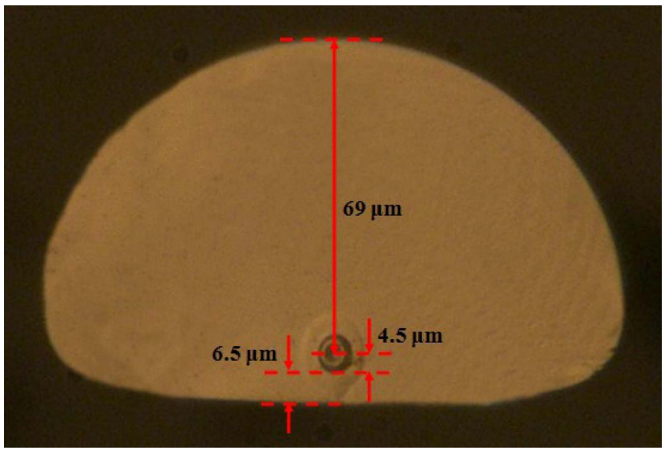

Fig. 1. Cross-section of the D-shaped fiber after etching by HF (15%) for 3 min.

where $n_{co}^{eff}(\lambda_i)$ and $n_{cl}^{eff}\lambda_i$ are the effective indices of the core mode and the *i*th cladding mode, respectively, and Λ is the grating period. For LPFG within a weakly guiding circular fiber, the effective index of the core mode is determined by the indices of the core and cladding, while the effective indices of the cladding modes are derived from the indices of cladding and external materials. When the index of the cladding is higher than that of the external material, the effective index of the *i*th cladding mode varies due to the change of the index of the external material; thus, the resonant wavelength for coupling between the core mode and the cladding mode shifts else well [26]. By selecting the cladding modes that is more sensitive to the external material, the higher sensitivity sensor can be realized. For a specific cladding mode, previous works show that the smaller the radius of the cladding is, the higher sensitivity of the LPFG to external material index is, owing to the increment of evanescent field outside of the fiber [20]. If the index of the cladding is lower than that of the external material, the resonant wavelength no longer shifts, but the attenuation of the resonant dip deepens as the increase of the external index [25].

The application of D-shaped fiber is an effective way to intensity evanescent field for high sensitivity sensors. By removing part of the cladding with polishing or etching, the core is much closer to the fiber flat surface, and the evanescent field of the guiding mode interacts directly with the surroundings; thus, the sensitivity of sensor prompted a lot [20]. Compared with the ordinary fibers [7], [9], [11], the key feature of D-shaped fiber with LPFG is side polishing or etching technology leading to a smaller distance between the flat surface and the fiber center (DFSFC) in the functional side, and this could enhance the sensitivity, as well as maintain the mechanical strength in contrast to drawing the fiber to micrometers [13], which is necessary for sensing. The DFSFC utilized in this paper is about 11 μm; thus, the predicted sensitivity is much higher than in the ordinary one.

Regarding to LGFG in a D-shaped fiber, the index of the core mode is not only determined by core and cladding but also determined by surroundings when the DFSFC is small enough. As the RI of the surroundings keeps changing, the resonant wavelength is the result of both core and cladding modes together; the RI sensitivity is the net result of the two effects. According to the experiments, we fabricate LPFG in a D-shaped fiber based on the thermal shock effect of focused high-frequency CO_2 laser pulses [22]–[24]. Due to its asymmetry index distribution induced by the laser exposure, we adjust the laser beam perpendicular to the flat surface of the D-shaped fiber in order to get higher sensitivity because the evanescent field could be enlarged much more in the direction.

Fig. 1 shows the cross section of the D-shaped fiber utilized in this paper, provided by Xiamen University, China. To make such a D-shaped fiber, first, the cladding of a single-mode fiber preform produced by a modified chemical vapor deposition method was partially polished off so that its cross section is D-shaped. After that process, the preform was polished carefully to make sure that the flat surface is smooth enough to prevent scattering; then, it was drawn in flame with high

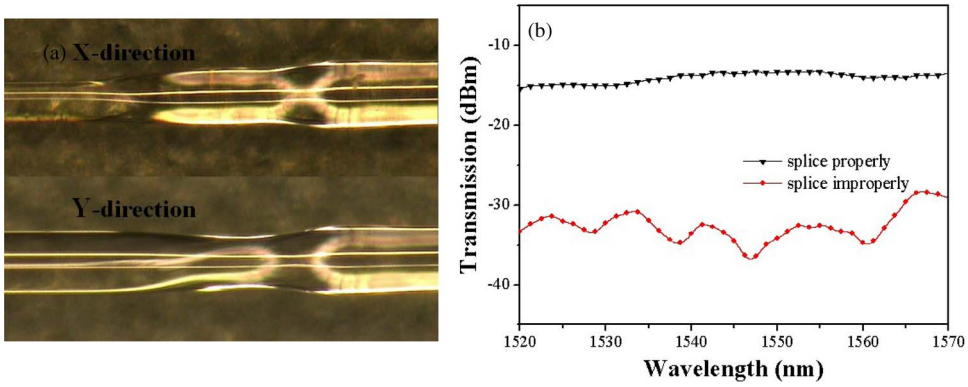

Fig. 2. (a) Splice image between D-shaped fiber and SMF in x and *y*-direction. (b) Transmission spectra of splicing D-shaped fiber between two SMF fibers under different situations.

temperature. In our experiment, we etched the cross section of the D-shaped fiber with hydrofluoric acid (HF) for 3 min. As we can see, the distance of the core layer from the flat surface is about 6.5 μm, intensifying the evanescent field while maintaining low loss. The indices of the cladding and core for the D-shaped fiber are 1.450 and 1.458, respectively.

As the LPFG written in a D-shaped fiber is exposed to the external magnetic field, it is worth to give the detailed information about MF used in our experiment. The diameter of ferromagnetic particles dispersing steadily in the liquid carrier with the aid of surfactant is around 10 nm, such as Fe_3O_4, $CoFe_2O_4$ [7]. After applying different magnetic fields to MF, the particles will be clustered to various structural patterns, exhibiting special optical properties, such as RI [27]. This property can be explained by effective dielectric constant calculation method [28], where RI is mainly interpreted by the equivalent dielectric constant ε with the definition of RI as $n = \varepsilon^{1/2}$. In particular, the RI of MF is varied monotonously with the change of applied magnetic-field intensity. Based on the magneto-controlled-RI property, we can detect magnetic field by measuring the RI-dependent parameters. Additionally, as the types of nanoparticles exhibit lower transmission loss than that of the other, water-based MF with nanoparticles is utilized in our experiment.

In this paper, we utilize water-based MF (*EMG 605, Ferrotec Co., Ltd., USA*), with particle density of 1.18 g/cm3 (25 °C) and viscosity of 5 mPa · s (27 °C), as the external surroundings. The RI of the MF is estimated to be around 1.40 when no magnetic field is applied [13], which is close to the cladding index of the D-shaped fiber.

3. Experimental Results and Discussion

3.1. Fabrication of LPFG in D-Shaped Fiber

As shown in Fig. 1, although the diameter of the core is very close to that of the single-mode fiber (SMF; *SMF-28, Corning Inc.*) used in our experiment, the mode field diameters of D-shape and SMF-28 fibers are different because of the asymmetric structure of the former one. If the exited cladding-mode energy is large enough at splicing point, the intermodal interference will occur when one short D-shape fiber is spliced between two SMF-28 fibers. In our experiment, the intermodal interference is avoided by precise axial offsetting to reduce the exited cladding-mode energy. And the splicing image within two orthogonal directions is shown in Fig. 2(a) after the end faces of the fibers are fused by several times of discharging. Fig. 2(b) shows the transmission spectra of the spliced structures with and without interference phenomena. All fibers are spliced by using a conventional splice machine (*S176, Furukawa Company, Ltd.*), and the minimize splice loss can be low to $\sim$9 dB in air while maintaining high strength.

Fig. 3 shows the schematic of the experimental setup for fabricating LPFG in D-shaped fibers. A section of the D-shaped fiber with 2.1 cm is spliced between two SMF-28 fibers by using the splicing method mentioned above, and two ends of the SMF-28 fibers are mounted on the centers of two

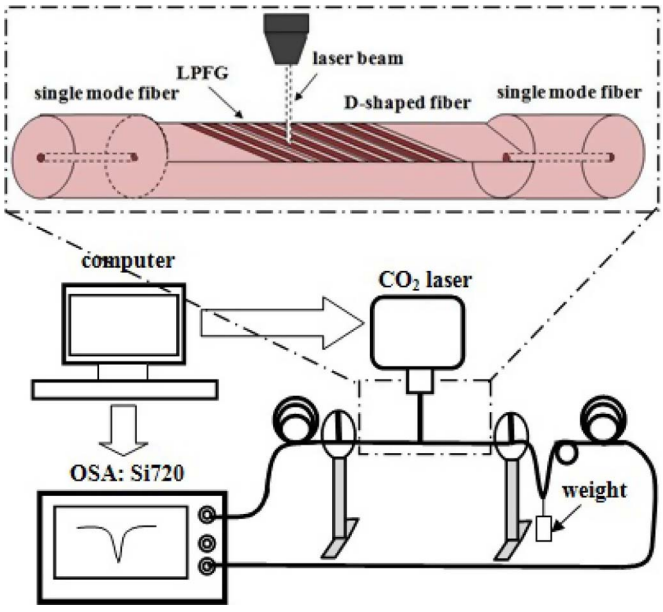

Fig. 3. Schematic of the system for fabricating LPFG in D-shaped fiber.

rotating disks, respectively. The fiber is loaded with a small weight (~30 g) to provide a prestress to the D-shaped fiber. An optical spectrum analyzer (OSA; *Si720, Micro Optics, USA*) with a wavelength resolution of 0.002 nm is used to measure the transmission spectra of the LPFG. By rotating the disks properly, the flat surface of the D-shaped fiber is adjusted to be perpendicular to the laser beam. As the focused laser pulses controlled by a computer are scanned transversely and longitudinally in the D-shaped fiber, LPFG are manufactured after several cycles of scanning [22], [24].

The details of the parameters for the CO_2 laser are the following: repetition rate of 10 kHz, the average power of ~0.35 W, the CO_2 beam spot of ~100 μm in diameter, and the temperature of 24 °C.

Although the calculation method [5] of the resonant wavelength for grating on D-shape is not precise enough, the resonant wavelength shift direction and the rough values could be concluded by the experimental results based on the normal phase-matching theory [5]. Due to the limited spectra range of light source and OSA, although we cannot observe the detail transmission spectra for the LPFG in D-shape fiber when outer RI changes from 1.0 to 1.45, we can select the proper period to optimize the spectrum in MF to test the wavelength shift in C-band when the applied magnetic field is applied. In our experiments, we fabricated many LPFGs in D-shaped fiber with different periods, and we concluded from the experimental results that the resonant wavelength with a period of ~685 μm in air will locate around 1580 nm, and when the outer RI changes from 1.0 to ~1.45, the resonant wavelength of grating will shift to ~1525 nm. Fig. 4 shows the measured transmission spectra of LPFG in a D-shaped fiber when the outer cladding is air and MF, respectively. Also, the transmission spectrum before the LPFG is fabricated is also shown in Fig. 4. As we can see, the resonant wavelength in air is beyond the spectral range of the OSA. When the outer RI of grating increases (e.g., replace air by MF), the resonant wavelength shifts to the shorter direction.

3.2. Experimental Results on Magnetic Sensing

After the grating fabrication, the LPFG is positioned into the center of a capillary tuber with an inner diameter of 1 mm and 100-mm length. As shown in Fig. 5, the fiber is held straight and parallel to the sections of the magnetic-field generator; thus, the magnetic field is perpendicular to the LPFG. The tube is filled with MF and sealed with candle grease to preventing flowing out and evaporation of MF while maintaining the tension of the fiber. By tuning the driving voltage, the different magnetic-field intensities could be generated by the magnetic generator (custom made by *Beijing Enerine Machinery Equipment Company, Ltd.*), and both changes in strength and wavelength of the attenuation for

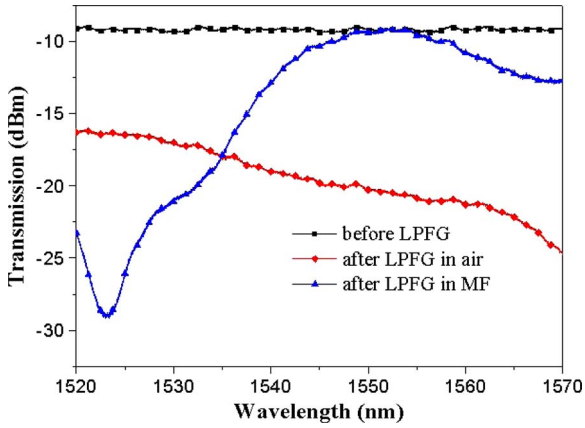

Fig. 4. Transmission spectra of the system before LPFG fabrication, after LPFG fabrication in air and in MF.

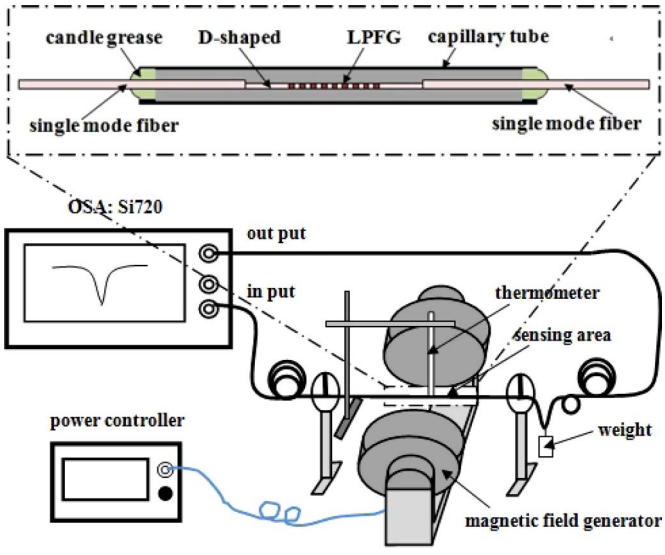

Fig. 5. Schematic diagram of the experimental setup for investigating the properties of the sensor.

the LPFG are recorded by the OSA. The magnetic-field intensity is measured using a portable magnetic meter (*HT20, Shanghai Hengtong Magnetic Company, Ltd.*).

To investigate the time response characteristics of the structure, we employ a tunable laser source with the power of 0 dBm and wavelength at 1544.0 nm to transmit the LPFG with period of 685 μm, and we utilize the detector (*InGaAs p-i-n photodiode 2053, New Focus, Inc.*) to detect the output intensity. The indications of the magnetic meter and the output power are recorded every second. As shown in Fig. 6, the rising and falling times are about 3.5 s and 3 s, respectively, and those are attributed to the characters of the magnetic generator and magnetic meter together. The rising and falling times for the sensor at 1544.0 nm when the applied magnetic field is 152.2 mT are about 5 s and 8 s, separately. This is mainly due to the high viscosity of the MF we used, and those parameters can be decreased by choosing MF with lower viscosity.

Considering the time response of the system, we record the spectra of the OSA 10 s after the application of the magnetic field. The magnetic-field step is about 20 mT, and the results are shown in Fig. 7. As shown, there are redshifts in the transmission spectra when the applied magnetic-field intensity increases, revealing that the RI of the MF decreases as the magnetic-field intensity increases, which is in accord to the previous report [9].

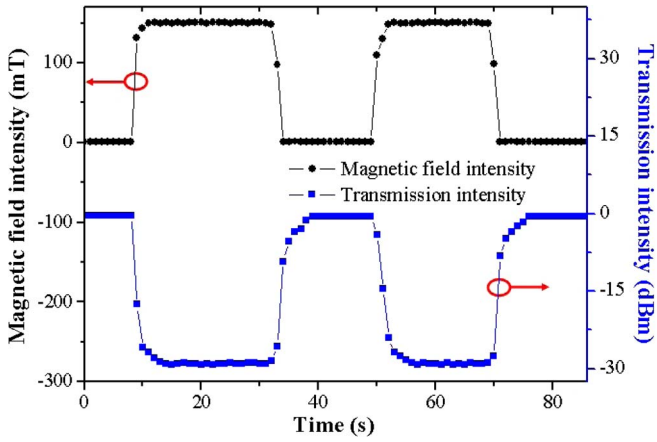

Fig. 6. Time response of the sensor at a wavelength of 1544.0 nm when the applied magnetic-field intensity is 152.2 mT.

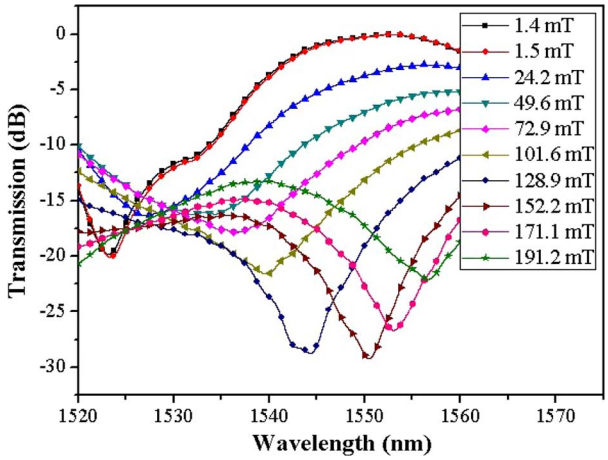

Fig. 7. Transmission spectra of the sensor at different magnetic-field intensities.

As the magnetic particles in the MF are affected by the applied magnetic field, hysteresis effect cannot be ignored. Therefore, we measured the spectra when the applied magnetic field decreases, and the resonant wavelength and attenuation at resonant wavelength versus the applied magnetic field are plotted in Fig. 8(a). By recording spectra every 10 s in decreasing the magnetic field, we found that the resonant wavelength cannot return to the original wavelength where no magnetic field is applied. Yet, after the applied magnetic field decreases to zero for 35 s, the resonant wavelength shifts to the original. In Fig. 7, the maximum resonant wavelength shift of 33.46 nm is observed by an increment of magnetic-field intensity as 189.7 mT. Thus, the sensitivity as high as 176.4 pm/mT is obtained.

3.3. Discussion

3.3.1. High Sensitivity and Linearity

As mentioned before, there are mainly two possible reasons to realize the high sensitivity compared with previous reports [9], [13]. First, the small difference between the RI of MF and the cladding index of the D-shaped fiber may generate high sensitivity. However, the MF utilized by Konstantaki *et al.* is the same as ours [13], while their resonant wavelength shifts only 7.5 nm, which

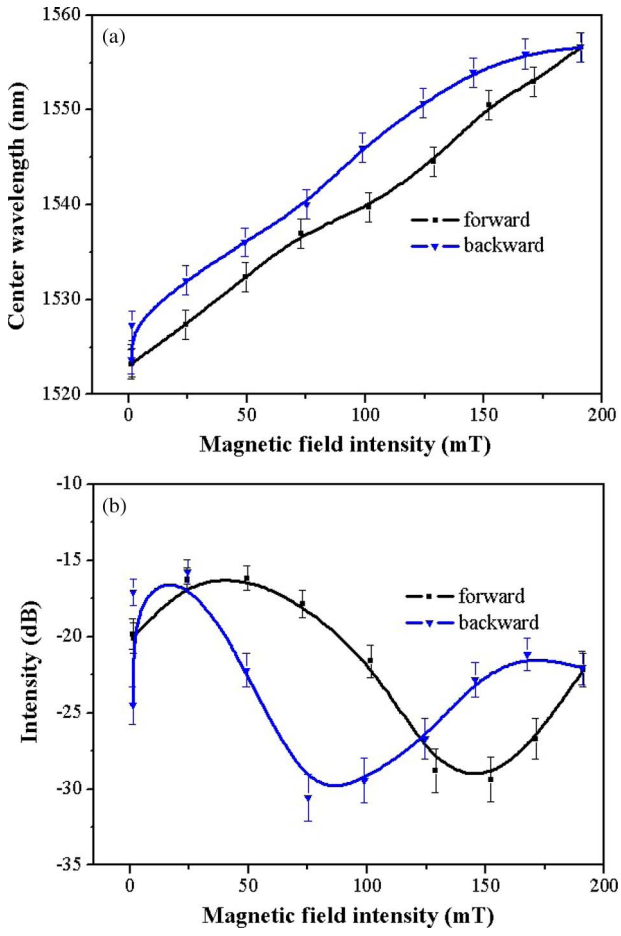

Fig. 8. (a) Resonant wavelength shift dependence on external magnetic field. (b) Resonant wavelength intensity dependence on external magnetic field.

implies that the MF is not the only reason. Second, the smaller cladding radius of the D-shaped fiber produces a higher sensitivity. Compared with the results of an ordinary LPFG coated with MF as the ambient media in [9], our sensitivity is about four times higher as that of 45.6 pm/mT, revealing that LPFG within a D-shaped fiber produces high sensitivity, which is demonstrated in [19] and [20]. In addition, the sensitivity could be enhanced by choosing coupling between core mode and the higher cladding mode or etching the D-shaped fiber with hydrofluoric acid.

As shown in Fig. 8(a), the response of the resonant wavelength is linear when the magnetic-field intensity is less than 100 mT, while it is nonlinear after that. This is mainly due to the fact that the higher magnetic-field intensity results in lower RI, which is less than the cladding index of the D-shaped fiber; thus, the sensitivity of the LPFG is nonlinear for itself [26]. Compared with the result in [21], which is not linear but an approximately exponential, our structure is easier to be demodulated with a conventional system. Besides, considering the good linearity, our structure would perform better in a larger measurement range of magnetic field. So, the characteristics of our structure are very important for industrial applications.

3.3.2. Hysteresis

By measuring the repeatability of the system, we increase and decrease the applied magnetic field for many times, and the hysteresis effect appears in all cycles. Compared with the hysteresis reported in [13], our hysteresis loop is more open, and it is may be the result of higher sensitivity and applied magnetic-field intensity. As the existence of viscosity for the MF, this hysteresis effect

cannot be eliminated but could be reduced by changing the magnetic field more slowly [29]. In addition, although the spectrum cannot return to the initial state in 10 s, due to the existence of hysteresis effect of MF, the resonant wavelength shifts to the original after 35 s. Considering the temporal characteristic of this structure, it can be utilized for dc magnetic-field sensing or in fields that the changing rate of magnetic field is relatively slow. The detail characteristic of the hysteresis on the system will be studied further in the next stage.

3.3.3. Attenuation Dip

It is shown in Fig. 8(b) that the change in depth of the attenuation dip under different magnetic-field intensities is approximately sinusoidal with the increase of the applied magnetic field. This can be explained by works in [22], where the coupling between the core mode and the cladding mode vary as the conditions of coupling changes, and the transmission for the resonant wavelength can be expressed as $\cos^2(K_m L)$, where K_m is the coupling coefficient of the core mode and the cladding mode, and L is the length of the grating. For the case of $0 < K_m L < \pi/2$, LPFG is undercoupling, while it is overcoupling for $\pi/2 < K_m L < \pi$. Thus, the attenuation dip is varied sinusoidally as the change of the external index. By changing the magnetic-field intensity, the RI of MF varies, and the undercoupling and overcoupling appear and disappear alternatively, due to their matching condition. Moreover, due to the hysteresis effect, the response for the forward and backward periods are different for a specific wavelength, while their shapes are almost the same, and this phenomenon appears in all the cycles.

As a result, after exposing the sensing part, which is not sealed by the candle grease, in air for two hours, the resonant wavelength no longer shifts, but the attenuation dip becomes shallow with the increase of the applied magnetic field, implying that the external RI is higher than the cladding RI for this moment. All those phenomena are in good agreement with the theory mentioned above.

4. Conclusion

In summary, we have proposed a highly sensitive magnetic sensor utilizing LPFG within a D-shaped fiber and the magneto-optical effect of the MF. The shift of the resonant wavelength with the variation of the external magnetic-field intensity has been studied in detail. The redshift of resonant wavelength is as high as 33.46 nm when the external magnetic-field intensity increased to 189.7 mT, resulting to a sensitivity of 176.4 pm/mT. The hysteresis effect is observed and explained by the characters of the MF. In addition, the sensor has advantages of electronic immunity, good mechanical strength, and low-cost fabrication process, making it attractive for magnetic sensing in harsh environments.

References

[1] J. E. Lenz, "A review of magnetic sensors," *Proc. IEEE*, vol. 78, no. 6, pp. 973–989, Jun. 1990.
[2] K. Mohri, T. Uchiyama, L. P. Shen, C. M. Cai, and L. V. Panina, "Sensitive micro magnetic sensor family utilizing magneto-impedance (MI) and stress-impedance (SI) effects for intelligent measurements and controls," *Sens. Actuators A, Phys.*, vol. 91, no. 1/2, pp. 85–90, Jun. 2001.
[3] Y. J. Rao, "In-fiber Bragg grating sensors," *Meas. Sci. Technol.*, vol. 8, no. 4, pp. 355–375, Apr. 1997.
[4] A. Yariv and H. V. Winsor, "Proposal for the detection of magnetic fields through magnetostrictive perturbation of optical fibers," *Opt. Lett.*, vol. 5, no. 3, pp. 87–89, Mar. 1980.
[5] H. J. Patrick, A. D. Kersey, and F. Bucholtz, "Analysis of the response of long-period fiber gratings to external index of refraction," *J. Lightw. Technol.*, vol. 16, no. 9, pp. 1606–1612, Sep. 1998.
[6] V. M. N. Passaro, F. Dell'Olio, and F. D. Leonardis, "Electromagnetic field photonic sensors," *Prog. Quantum Electron.*, vol. 30, no. 2/3, pp. 45–73, Jan. 2006.
[7] H. E. Horng, C.-Y. Hong, and H. C. Yang, "Designing the refractive indices by using magnetic fluids," *Appl. Phys. Lett.*, vol. 82, no. 15, pp. 2434–2436, Apr. 2003.
[8] H. Okamura, "Fiber-optic magnetic sensor utilizing the Lorentzian force," *J. Lightw. Technol.*, vol. 8, no. 10, pp. 1558–1564, Oct. 1990.
[9] T. Liu, X. F. Chen, Z. Y. Di, and J. F. Zhang, "Tunable magneto-optical wavelength filter of long-period fiber grating with magnetic fluids," *Appl. Phys. Lett.*, vol. 91, no. 12, pp. 121116-1–121116-3, Sep. 2007.
[10] J. L. Arce-Diego, R. Lüpez-Ruisanchez, and J. M. López-Higuera, "Fiber Bragg grating as an optical filter tuned by a magnetic field," *Opt. Lett.*, vol. 22, no. 9, pp. 603–605, May 1997.

[11] H. V. Thakur, S. M. Nalawade, S. Gupta, R. Kitture, and S. N. Kale, "Photonic crystal fiber injected with Fe_3O_4 nanofluid for magnetic field detection," *Appl. Phys. Lett.*, vol. 99, no. 16, pp. 161101-1–161101-3, Oct. 2011.
[12] P. Zu, C. C. Chan, W. S. Lew, Y. X. Jin, Y. F. Zhang, H. F. Liew, L. H. Chen, W. C. Wong, and X. Y. Dong, "Magneto-optical fiber sensor based on magnetic field," *Opt. Lett.*, vol. 37, no. 3, pp. 398–400, Feb. 2012.
[13] M. Konstantaki, A. Candiani, and S. Pissadakis, "Optical fibre long period grating spectral actuators utilizing ferrofluids as outclading overlayers," *J. Eur. Opt. Soc. Rap. Public.*, vol. 6, pp. 11007-1–11007-6, Mar. 2011.
[14] H. E. Horng, J. J. Chieh, Y. H. Chao, and S. Y. Yang, "Designing optical-fiber modulators by using magnetic fluids," *Opt. Lett.*, vol. 30, no. 5, pp. 543–545, Mar. 2005.
[15] S. L. Pu, X. F. Chen, Y. P. Chen, Y. H. Xu, W. J. Liao, L. J. hen, and Y. X. Xia, "Fiber-optic evanescent field modulator using a magnetic fluid as the cladding," *J. Appl. Phys.*, vol. 99, no. 9, pp. 093516-1–093516-4, May 2006.
[16] L. Shi, X. F. Chen, H. J. Liu, Y. P. Chen, Z. Q. Ye, W. J. Liao, and Y. X. Xia, "Fabrication of submicron-diameter silica fibers using electric strip heater," *Opt. Exp.*, vol. 14, no. 12, pp. 5055–5060, Jun. 2006.
[17] P. Mach, M. Dolinski, K. W. Baldwin, J. A. Rogers, C. Kerbage, R. S. Windeler, and B. J. Eggleton, "Tunable microfluidic optical fiber," *Appl. Phys. Lett.*, vol. 80, no. 23, pp. 4294–4296, Jun. 2002.
[18] S. T. Huntington, K. A. Nugent, P. Mulvaney, K. M. Lo, and A. Roberts, "Field characterization of a D-shaped optical fiber using scanning near-field optical microscopy," *J. Appl. Phys.*, vol. 82, no. 2, pp. 510–513, Jul. 1997.
[19] X. Chen, K. Zhou, L. Zhang, and I. Bennion, "Optical chemsensors utilizing long-period fiber gratings UV-inscribed in D-fiber with enhanced sensitivity through cladding etching," *IEEE Photon. Technol. Lett.*, vol. 16, no. 5, pp. 1352–1354, May 2004.
[20] H. J. Kim, O. J. Kown, S. B. Lee, and Y. G. Han, "Measurement of temperature and refractive index based on surface long-period gratings deposited onto a D-shaped photonic crystal fiber," *Appl. Phys. B*, vol. 102, no. 1, pp. 81–85, Jan. 2011.
[21] C. L. Tien, T. W. Lin, C. C. Hwang, and W. F. Liu, "Magnetic field sensors based on D-shaped long period fiber gratings," in *Proc. SPIE*, 2002, vol. 7508, pp. 750811-1–750811-6.
[22] Y. J. Rao, T. Zhu, Z. L. Ran, Y. P. Wang, J. Jiang, and A. Z. Hu, "Novel long-period fiber gratings written by high-frequency CO_2 laser pulses and applications in optical fibre communication," *Opt. Commun.*, vol. 229, no. 1–6, pp. 209–221, Jan. 2004.
[23] T. Zhu, Y. J. Rao, J. L. Wang, and Y. Song, "A highly sensitive fiber-optic refractive index sensor based on an edge-written long-period fiber grating," *IEEE Photon. Technol. Lett.*, vol. 19, no. 24, pp. 1946–1948, Dec. 2007.
[24] T. Zhu, K. S. Chiang, Y. J. Rao, Y. Song, C. H. Shi, and M. Liu, "Characterization of long-period fiber gratings written by CO_2 laser in twisted single-mode fibers," *J. Lightw. Technol.*, vol. 27, no. 21, pp. 4863–4869, Nov. 2009.
[25] T. Erdogan, "Fiber grating spectra," *J. Lightw. Technol.*, vol. 15, no. 8, pp. 1277–1294, Aug. 1997.
[26] K. S. Chiang, Y. Q. Liu, M. N. Ng, and X. Y. Dong, "Analysis of etched long-period fibre grating and its response to external refractive index," *Electron. Lett.*, vol. 36, no. 11, pp. 966–967, May 2000.
[27] T. Hu, Y. Zhao, X. Li, J. J. Chen, and Z. W. Lv, "Novel optical filter current sensor based on magnetic fluid," *Chin. Opt. Lett.*, vol. 8, no. 4, pp. 392–394, Apr. 2010.
[28] D. J. Bergman, "The dielectric constant of a composite material—A problem in classical physics," *Phys. Rep.*, vol. 43, no. 9, pp. 377–407, Jul. 1978.
[29] D. C. Jiles and D. L. Atherton, "Theory of ferromagnetic hysteresis," *J. Magn. Magn. Mater.*, vol. 61, no. 1/2, pp. 48–60, Sep. 1986.